Separating Inherent Asymmetries from High Sensitivity Rotor Bar Fault Indicator

Goran Stojičić, Peter Nussbaumer, Gojko Joksimović, Mario Vašak, Nedjeljko Perić, Thomas M. Wolbank

Abstract – **Inverter operation significantly reduces sensitivity of rotor bar detection methods based on current signature analysis (CSA). Considering the high frequency and transient electrical properties of the machine a very sensitive detection was proven possible by different authors recently. These methods apply high frequency or transient voltage signals to the machine terminals using the inverter and measure the current reaction. For on-line detection however these high frequency and transient electrical properties are usually superposed with inherent asymmetries like slotting or spatial saturation. To ensure a fault detection in all operating states and to keep sensitivity high the flux/load dependencies of these inherent asymmetries have to be identified during a pre commissioning procedure using for example neural network approach. After this procedure an accurate compensation is possible in all operating states. In this paper a measurement and signal processing chain is described to directly separate the different inherent asymmetries from the fault induced asymmetry without pre commissioning. This signal processing chain is based on repetitive data sampling during normal operation of the drive and applying a set of Fourier transforms. Measurements on a special manufactured machine are presented. The cage of the test rotor allows a single replacement of each individual bar thus enabling to investigate the effect of even partially broken bars. Measurement results prove the efficiency of the proposed method to accurately eliminate the inherent asymmetries caused by slotting and spatial saturation in various points of operation.**

Index Terms-- AC motor drives, Discrete Fourier transform, Fault diagnosis, Harmonic analysis, Induction motor protection, Monitoring, Pulse width modulated inverters, Squirrel cage motors, Switching transients, Transient response

I. INTRODUCTION

NOWADAYS inverter fed variable speed drives are more or less standard in modern industrial drive applications and the maximum power is steadily increasing to levels clearly above 1 MW. Dynamic properties are excellent when operated under field oriented control. One drawback of this configuration is the additional stress put to machine components like insulation or bearings resulting from the combination of dynamic operation, pulse width modulation (PWM) and fast switching power electronics.

As investigations of drive reliability have shown rotor cage defect are responsible for about 10% of all drive breakdowns [1]-[2]. While induction machines with higher power rating usually have brazed copper cages that are more robust, low power machines are manufactured using die cast technique in combination with aluminum and copper. As a result of non ideal die casting process together with the difference of the lamination steel and the aluminum or copper with respect to the coefficient of thermal expansion machines thermal fatigue cycles may deteriorate the structure of the cage. Especially machines of low power rating are thus more frequently affected from rotor defects [3].

Much work has been done in the field of broken rotor bar detection recently as reported in [4].

Mains fed operation was the aim of the majority of the published methods in the past. As a consequence the side bands in the stator current are considered the dominant fault indicator leading to a group of methods that are also denoted current signature analysis (CSA) in literature. The ways to extract the fault indicators from the measured signal are based on algorithms of Fourier [5]-[6] or wavelet transform [7]-[8]. In addition also neural network approaches [9], [10], genetic algorithms [11] and signal processing techniques derived form pattern recognition [12] are proposed.

Detection sensitivity of CSA based methods is high when machine is fed by ideal sinusoidal voltages and under steady state operating conditions. Issues of changing load levels and asymmetrical supply voltages are frequently addressed by neural network, genetic algorithm and/or the additional measurement of supply voltage.

Considering inverter operation under variable frequency, accuracy is further decreased and a detection usually only possible under steady state frequency and load.

Detection of the side bands or even the fundamental wave frequency in the presence of inverter non-linearity, the frequencies introduced by the pulse width modulation (PWM) method and the control loops for current, speed and/or position gets really difficult.

As a consequence a separate group of methods is proposed able to handle the disturbing effects of inverter operation.

This work was supported in part by the European Union under the SEE-ERA.NET Framework Grant No. ERA-80.

Goran Stojičić is with the Department of Energy Systems and Electrical Drives, Vienna University of Technology, Vienna, Austria (e-mail:goran.stojicic@tuwien.ac.at)

Peter Nussbaumer is with the Department of Energy Systems and Electrical Drives, Vienna University of Technology, Vienna, Austria (e-mail:peter.nussbaumer@tuwien.ac.at)

Gojko Joksimović is with the Faculty of Electrical Engineering, University of Montenegro Podgorica, Montenegro (e-mail:joxo@ac.me)

Mario Vašak is with the Faculty of Electrical Engineering and Computing, University of Zagreb, Croatia (e-mail: mario.vasak@fer.hr)

Nedjeljko Perić is with the Faculty of Electrical Engineering and Computing, University of Zagreb, Croatia (e-mail: nedjeljko.peric@fer.hr)

Thomas M. Wolbank is with the Department of Energy Systems and Electrical Drives, Vienna University of Technology, Vienna, Austria (e-mail: thomas.wolbank@tuwien.ac.at)

978-1-4244-9303-6/11/$26.00 ©2011 IEEE

The space phasor of the stator current is measured and transferred to the rotor fixed reference frame where the modulus of the phasor is independent of the machine's fundamental wave frequency [13], [14]. As a consequence the masking of the two slip-related side bands by the fundamental wave is eliminated.

Wiegner distribution enables the detection at slow changing stator frequency [15]. Torque pulsations introduced by the fault are detected in [16].

A comparison of the machine torque calculated by fundamental wave models is performed to extract a fault indicator in [17]. In [18] rotor defects are detected using the virtual current of a fundamental wave model.

All of the methods mentioned are based on the interaction of the defect bar with the machine's fundamental wave. As a consequence a minimum load level of around 30% is needed to detect the rotor asymmetries. Methods able to detect faults at zero load are presented in [19]-[22], some are however limited to off-line measurements.

From the customer side a high sensitivity is usually demanded in order to detect a defect in an early stage and also without limitation to the machine operating state.

To achieve this usually the 'healthy' machine has to be identified during a commissioning stage to set all the threshold values and to eliminate load and speed dependent disturbances.

The method presented in the following is based on an online identification of the machine transient reactances. While the extraction of a very precise fault indicator is possible at low or zero load, the indicator is superposed with disturbing signal components when the machine is loaded. To keep the sensitivity high it is thus necessary to identify the disturbing components during commissioning. The signal processing proposed here enables a separation of the fault induced signal component from all disturbing components of the 'healthy' machine without any knowledge of the machine parameters and without any test measurements. High sensitive detection of rotor bar faults is thus possible in all operating states.

II. Online Estimation of the Transient Leakage Inductance

In the following, the structure and signal processing necessary to carry out the measurements is explained. A more detailed description is given in [23].

The standard way of identifying the dynamic parameters of a system is to observe the step response. In case of an electrical machine the step excitation can be easily realized using the dc link of the voltage source inverter. When changing the inverter output state from inactive to any active switching state a step is applied to the machine terminals with a magnitude equal to the dc link voltage. The system response can be detected using the built-in current sensors of the inverter.

Assuming an ideal symmetrical machine the step response can be calculated using the stator equation of the machine (1).

$$\underline{v}_S = r_S \cdot \underline{i}_S + l_l \cdot \frac{d\underline{i}_S}{d\tau} + \frac{d\underline{\lambda}_R}{d\tau} \tag{1}$$

The three voltage drops influencing the current reaction of the machine are influenced by the parameters stator resistance r_S, leakage inductance l_l, and the back emf (time derivative of the rotor flux $\underline{\lambda}_R$).

In the first transient reaction to the voltage step (some ten µs) the dominant voltage drop will be the transient leakage times the time derivative of the current and eventually the back emf (if the machine is running at high speed). An accurate identification of the transient leakage inductance is thus only possible after eliminating the possible influence of the back emf.

This elimination can be realized by evaluating the step responses of two voltage steps with different inverter output states. If these two output states are subsequent the fundamental wave point of operation and especially the direction and magnitude of the back emf will not change significantly. In addition the dc link voltage can be considered constant during the short time period of the pulses.

If the voltage pulses and the sampled current reaction of the two inverter output states are denoted with the indexes I and II the following equations are obtained.

The fundamental wave point of operation of the stator current $\underline{i}_S$ as well as its time derivative can be directly measured. The back emf does not change significantly between the two subsequent pulse excitations thus its influence is eliminated by simply subtracting the two equations (denoted with index *I* and *II*). The same applies for the influence of the stator resistance.

Up to now an ideal symmetrical machine has been assumed with the leakage inductance l_l equal the transient inductance according to (1).

As the transient inductance of the machine differs from the fundamental wave leakage it is denoted $l_{l,t}$ in the following.

$$\underline{v}_{S,I} - \underline{v}_{S,II} = l_{l,t}\left(\frac{d\underline{i}_{S,I}}{d\tau} - \frac{d\underline{i}_{S,II}}{d\tau}\right) \tag{2}$$

If in a machine a fault is developing it will no longer be symmetrical. Due to the existing asymmetry the parameter of the transient leakage must thus be changed from a scalar value in (2) into a complex one. Now the directions of applied pulse voltage ($\underline{v}_{S,I}$-$\underline{v}_{S,II}$) and the resulting current time derivative (slope) will no longer be the same.

This complex transient leakage inductance $\underline{l}_{l,t}$ is composed of a scalar offset value l_{offset} and a complex value $\underline{l}_{mod}$. The offset value is representing the symmetrical machine while the complex value represents the fault induced asymmetry with its magnitude and spatial direction.

$$\underline{l}_{l,t} = l_{offset} + \underline{l}_{\mathrm{mod}}, \quad \underline{l}_{\mathrm{mod}} = l_{\mathrm{mod}} \cdot e^{j2\gamma} \tag{3}$$

The angle γ of the asymmetry portion gives the spatial position of the maximum inductance within one pole pair.

The asymmetry has a period of two with respect to one electrical revolution, which corresponds to the expected modulation of a rotor fault. The influence of a broken rotor bar on the transient leakage is repeated for every pole of the stator windings.

When applying a voltage pulse sequence and evaluating the current reaction the overall time derivative of the machine current can thus be separated into a 'symmetrical' portion determined by l_{offset} that corresponds to the scalar value $l_{l,l}$ and an 'asymmetrical' portion that is influenced by $\underline{l}_{\mathrm{mod}}$, leading to an angle-dependent cross-coupling.

Separating the value of $\underline{l}_{\mathrm{mod}}$ it is thus possible to determine magnitude and position of the asymmetry what, in case of a rotor bar defect corresponds to the position of the defect bar with respect to the stator windings and the severity of the bar defect (starting from only increased bar resistance of a single bar to one or even more broken bars).

The value of the transient inductance associated to the faultless machine l_{offset} can be identified in advance. Thus for the evaluation algorithm it is sufficient to monitor the resulting current slope of two switching states after elimination of stator resistance and back emf according to (2).

This leads to (4) where the complex conjugate is marked with *.

The measured current slope of the excitation sequence is thus directly influenced by the magnitude and position of $\underline{l}_{\mathrm{mod}}$ according to (4),

$$\frac{d\underline{i}_{S,I}}{d\tau} - \frac{d\underline{i}_{S,II}}{d\tau} = y_{offset} \cdot \left(\underline{v}_{S,I} - \underline{v}_{S,II}\right) + \underline{y}_{mod} \cdot \left(\underline{v}^*_{S,I} - \underline{v}^*_{S,II}\right) \quad (4)$$

with the values of y_{offset} and $\underline{y}_{mod}$ obtained from inversion as depicted in (5).

$$y_{offset} = \frac{l_{offset}}{l^2_{offset} - l^2_{mod}} \quad \underline{y}_{mod} = -\frac{l_{\mathrm{mod}}}{l^2_{offset} - l^2_{mod}} \cdot e^{j(2\gamma - 2\arg(\underline{v}_{S,I-II}))} \quad (5)$$

As can be seen in the previous equations the difference between the two inverter switching states determine the 'main' direction of the resulting current change. In symmetrical machines the value of y_{offset} is always clearly dominant with the magnitude of $\underline{y}_{mod}$ even for a faulted machine being only up to 10% of the symmetrical y_{offset}.

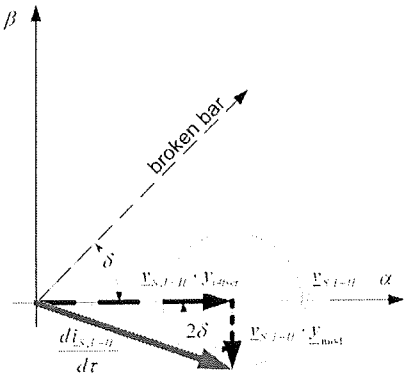

Fig. 1: Influence of y_{offset} and y_{mod} on the resulting transient current change for a given pulse sequence ($v_{S,I}$ - $v_{S,II}$= $v_{S,I-II}$). Asymmetry position assumed to 45°.

Assuming an ideal symmetrical machine only the inverse inductance y_{offset} influences the time derivative of the current leading to a measured current slope after signal processing (elimination of back emf according to (2)) in the horizontal direction (black dashed phasor).

In Fig. 1 the same resulting excitation direction and the symmetrical current slope are depicted together with an asymmetry caused by a broken bar. The position of the asymmetry is marked by the dashed black phasor denoted "broken bar" pointing in the direction of the maximum inductance. The angle δ(=45°) defines the spatial direction of the maximum transient inductance (broken bar) with respect to the direction of the resulting excitation voltage ($\underline{v}_{S,I-II}$) as indicated. To give a clearer geometrical impression of the influence of the fault induced asymmetry, the value of $\underline{y}_{mod}$ has been clearly increased with respect to y_{offset} in the figure.

As depicted the fault induced asymmetry leads to a current slope (black dotted) orthogonal to the direction of excitation corresponding to twice the angle of the asymmetry (45°).

The resulting current slope after the signal processing is thus the summation of the symmetrical and the fault induced portion. This phasor (red solid) is obtained from the excitation, measurement, and signal processing structure.

The asymmetry depicted (broken bar) is assumed to lead to an ideal sinusoidal distribution of the inductance with a period that equals twice that of one electrical revolution. If the direction of the asymmetry is the same or opposite as the direction of the resulting excitation voltage (δ=0°/180°), the resulting current slope obtained has the same direction as the applied resulting voltage as if the machine was symmetrical.

However, compared to the symmetrical machine its magnitude is either greater or smaller than for the symmetrical case.

The tip of the resulting phasor (red solid) moves along the dotted circle twice when the position of the broken bar (rotor) is changed over one electrical period.

The fault indicator signal can thus be obtained considering the modulation of the resulting current slope phasor with respect to the position of the fault induced asymmetry.

III. Measurement and Signal Processing

As was shown in the previous section the resulting current slope resulting from a pulse sequence shows a distinct modulation that contains the information on the machine's asymmetry. For exploitation of this information for high precision monitoring it is necessary to follow some specific signal processing steps.

Usually control electronics is used to generate both, the excitation and the trigger signals for the measurement. The easiest way for the excitation and the resulting signal processing is to apply a sequence of two active inverter switching states with some ten µs duration each. When the two generated voltage phasors point in opposite directions, the excitation axis and the resulting voltage phasor ($\underline{v}_{S,I-II}$) is always parallel with one phase axis.

The current time derivative is approximated by two current samples taken during each voltage pulse. Therefore a replacement of the continuous time derivative $di/d\tau$ by the difference $\Delta i_\sigma/\Delta\tau$ is possible.

The elimination of the back emf is done by subtraction of the two pulses (2). The resulting current slope obtained contains information of both the symmetrical as well as the asymmetrical portion of the inductance. In a real machine the allocation between symmetrical and fault induced part is 90% to 10%. Furthermore the symmetrical part is a function of the load level. It is thus necessary to clearly separate these two shares in the measured signal.

There are two options to determine or separate the share of the symmetrical inductance in the resulting signal. One is to identify its value in advance on the symmetrical, faultless machine. The parameters to be observed for the identification are the flux as well as the load level of the machine. The second option is to eliminate the symmetrical part using a voltage excitation that sequentially changes its direction in the three phases. Then it is possible to calculate one resulting phasor from three different spatial directions. The share of the symmetrical machine then leads to a zero sequence component that is eliminated.

After this step, the remaining phasor thus only contains information on the machine's asymmetry and is also denoted asymmetry phasor. Before it can finally be used as fault indicator it is however, necessary to apply some further signal processing.

The reason is that the asymmetry induced by a broken rotor bar is superposed by further inherent asymmetries, which are present in every machine even when healthy. These inherent asymmetries are caused by spatial saturation, slotting, rotor anisotropy. To ensure a high sensitivity, the detected asymmetry phasor has to be split up into the several components,. An identification and separation of these inherent asymmetries however, is possible as each of them has deterministic behavior.

A. Inherent asymmetries

As already described the asymmetry phasor is composed of several parts. The main asymmetry in healthy induction machines with skewed rotor is the saturation saliency. It is caused by different levels of saturation arising from the spatial distribution of the fundamental wave along the circumference. The modulation period equals twice that of the fundamental wave. This corresponds to the machine's number of poles. The magnitude of the saturation saliency depends on the flux and load level of the machine. Furthermore, there is also a dependence of its angular position with respect to the current phasor.

Another inherent asymmetry is caused by the openings of the slots in the lamination. The number of rotor slots determines the period of this modulation. The operation point has only marginally influence on this modulation. On a machine with closed rotor slots, that asymmetry is very small or even negligible.

In case of a rotor bar fault the modulation period of this asymmetry is the same as, or close to the modulation period of the saturation saliency depending on the load. For fault detection separation of the fault induced asymmetry and the saturation saliency has to be ensured. Therefore special signal processing steps are needed which will be described hereafter.

B. Signal processing for separation of inherent asymmetries

As already mentioned an asymmetry phasor can be detected for each point of operation (i.e. rotor position and flux position). In a first step a set of asymmetry phasors is collected each with a fixed flux position with respect to the stator. This set of measurements is arranged to form a full revolution of the rotor. This step is repeated for all flux positions with respect to the stator.

The resulting set of phasors is arranged to a two dimensional field further denoted as phasor matrix. Each field of this matrix now contains an asymmetry phasor for a certain rotor and flux position. Thereby rows of the phasor matrix contain all asymmetry phasors for one flux position, each with a different rotor position. On the other side columns contain all asymmetry phasors for one rotor position, each with a different flux position. The Fig. 2 schematically depicts the phasor matrix with its elements. In the upper left corner of the matrix, flux- and rotor angular positions are indicated by phasors.

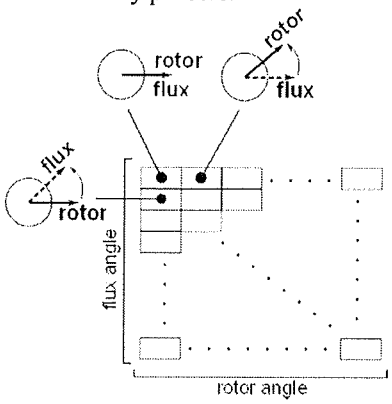

Fig. 2: Schematic diagram of the phasor matrix.

The data acquisition thus requires several signal processing steps. In Fig. 3 a block diagram of the whole signal processing is depicted. At first the control system initiates the fault examination. This leads to generation of test pulses (voltage pulses). During this pulses, current response measurement is done and the asymmetry phasor calculated. After that the asymmetry phasor, flux angle, and rotor angle are forwarded to the phasor matrix. Based on the angles of flux and rotor the position within the matrix is determined and the asymmetry phasor value is stored. Meanwhile rotor and flux angle have changed according to the point of operation. Test pulse generation, measurement, data acquisition then is repeated till the matrix is filled with data.

Subsequently a complex Fast Fourier Transformation (FFT) is done for each row of the matrix and clustered as indicated on the right side of Fig. 3.

As already described, the number of periods of the saturation saliency along the circumference equals the number of poles of the machine as saturation level is detected only, not its direction. On the other side a broken rotor bar leads to the same change in transient flux distribution under every pole. At zero or low load both asymmetries thus have the same or almost same period and have to be separated precisely to ensure high sensitivity.

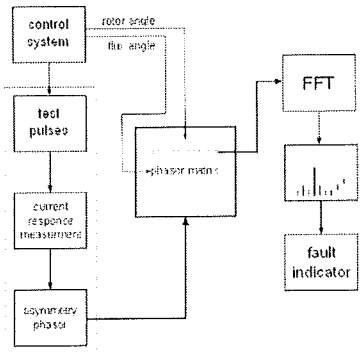

Fig. 3: Block diagram of measurement, signal processing and data acquisition.

The separation of these two parts is now realized by the phasor matrix. A FFT over one row represents the spatial distribution for a window length of one mechanical revolution and a fixed flux position. Thus the saturation saliency shifts to offset position caused by fixed flux position for each row. However, the number of the harmonic induced by the rotor bar fault equals the number of poles. The corresponding harmonic is also denoted fault harmonic in the following.

The fault indicator can finally be obtained from the fault harmonic of each row.

Basically one row of the matrix is sufficient for detecting rotor bar faults with very accuracy. However, in order to verify also the statistical properties of the fault indicator the whole matrix has been measured and evaluated in the next paragraph.

IV. Measurement Results and Detection Sensitivity

The measurement set up consists of a test machine, a voltage source inverter and a measurement and control unit realized by a computer system.

The test machine is a 5kW machine with 2 poles and 36 stator slots. The rotor is a specially designed and manufactured one, in order to enable a non-destructive realization of rotor asymmetries. The cage consists of 28 unskewed rotor bars made of solid copper and two copper end rings. This rotor design allows removing or changing each of the 28 rotor bars. Thus several fault configurations can be realized easily by removing or changing a copper bar to a bar made of another material. Unlike with a cast rotor cage, this rotor design allows an individual adjustment of rotor fault severity without destroying the rotor by drilling holes in the end rings or lamination.

The measurements were carried out using the control unit programmable under Matlab/Simulink. The excitation and data acquisition sequence was done as described in the previous section.

To produce a fault induced asymmetry the resistance of one rotor bar at least must be increased. For sensitivity verification of the investigated method, different fault cases were examined. Therefore one rotor bar was changed. The so done variation of the rotor bar resistance is done in five steps starting from symmetrical cage till the removal of a single bar. The different fault levels were obtained using bars made of copper, aluminum, brass and steel. The resulting increase of the bar resistance with respect to the solid copper bar is measured from +79% up to +762%. Table I shows the variation steps applied and their resistance levels.

As previously described, data acquisition/storage is done by a phasor matrix. Rows of the matrix represent different rotor positions (each for constant flux position) and columns different flux positions (each for constant rotor position). Flux angle is partitioned to 72 steps while the rotor position to 256 steps. Thus the matrix size is 72x256 elements. It has however to be stressed, that this high amount of data was only taken to show the overall properties of the method. Detection is already possible with only one row of much less than 256 elements.

TABLE I
Rotor Bars and their Resistance Increase Applied for the Measurements

	abs. resistance [Ω]	rel. res. increase [%]
copper	$44.1 \cdot 10^{-3}$	0
aluminum	$79.2 \cdot 10^{-3}$	+79
brass	$209.8 \cdot 10^{-3}$	+374
steel	$380.3 \cdot 10^{-3}$	+762
removed	-	-

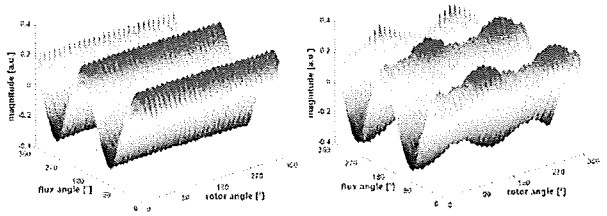

Fig. 4: Real part of phasor matrix at rated flux and 25% load. Left: faultless rotor, Right: rotor with one bar made of steel.

Fig. 4 depicts real values of the phasor matrix for two cases. Left diagram shows faultless case and right diagram rotor with implemented steel bar. All measurements were taken at rated flux and load level of 25%.

The horizontal axes represent flux angle and rotor angle respectively. The vertical axis displays magnitude of real asymmetry phasor value. If the two cases are compared than an increase of the fault harmonic (period equals number of poles) with respect to the rotor angle is well seen. The

modulation of the saturation harmonic is only visible when changing the flux angle.

The complex fault harmonics for all investigated fault cases are depicted in Fig. 5 as vectors. The faultless case serves as reference thus its value equals the zero vector (the point of origin). As can be seen, the removal of one bar (denoted 'broken') and the replacement of a copper bar with a steel bar lead to a very distinct change and a clear detection of a broken or almost broken bar.

On the other side the proposed measurement and signal processing method allow a very precise monitoring of rotor bar faults. Even a fault in the early stage can clearly be detected, as shown in the zoomed area near the origin where the results of a brass bar and an aluminum bar are located - still clearly distinguishable from the symmetrical rotor. Further measurements for different load levels have proven that the influence of load level is negligible.

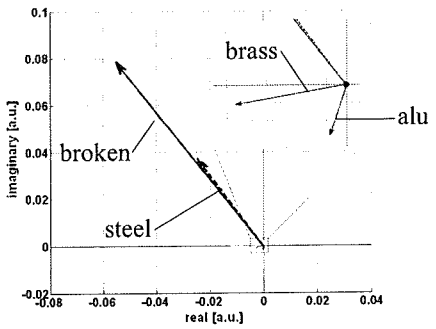

Fig. 5: Resulting fault indicator values for the investigated fault cases

V. CONCLUSIONS

This paper presents a new measurement and signal processing setup to calculate a fault indicator for rotor bar faults. It is based on transient excitation of the machine with voltage pulses. The resulting current response is measured and hence an asymmetry phasor is calculated which consists components originating from rotor bar asymmetries as well as inherent saliencies.

The asymmetry phasor values are collected for several rotor and flux positions in a phasor matrix. After a fast Fourier transformation the fault harmonic delivers the fault indicator while inherent saliencies reside as offset values or higher harmonics. Thus separation of rotor bar asymmetries and inherent asymmetries is performed and fault detection is established. The measurements have proven that even an increase of resistance in only a single bar of only 72% is still clearly noticeable. Thus rotor bar faults in an early stage are well detectable during normal operation of the drive.

VI. REFERENCES

[1] A. H. Bonnet, C. Yung, "Increased efficiency versus increased reliability," *IEEE Industry Applications Magazine*, vol.14, no.1, pp.29-36, 2008.

[2] IEEE Committee Report, "Report of large motor reliability survey of industrial and commercial installation, Part I and Part II," *IEEE Transactions on Industry Applications*, vol.21, no.4, pp.853–872, Jul./Aug. 1985

[3] M. Hodowanec, W. R. Finley, "Copper versus Aluminum - Which Construction is Best?," *IEEE Industry Applications Magazine*, vol.8, no.4, pp. 14-25, 2002

[4] A. Bellini, F. Filippetti, C. Tassoni, G. Capolino, "Advances in Diagnostic Techniques for Induction Machines," *IEEE Transactions on Industrial Electronics*, vol.55, no.12, pp.4109-4126, 2008

[5] W. Le Roux, R. G. Harley, T. G. Habetler, "Detecting Rotor Faults in Low Power Permanent Magnet Synchronous Machines," *IEEE Transactions on Power Electronics*, vol.22, no.1, pp.322-328, 2007

[6] A. Bellini, A. Yazidi, F. Filippetti, C. Rossi, G. Capolino, "High Frequency Resolution Techniques for Rotor Fault Detection of Induction Machines," *IEEE Transactions on Industrial Electronics*, vol.55, no.2, pp.4200-4209, 2008

[7] S.H. Kia, H. Henao, G. Capolino, "Diagnosis of Broken Bar Fault in Induction Machines Using Discrete Wavelet Transform without Slip Estimation," *IEEE Transactions on Industry Applications*, vol.45, no.4, pp.1395-1404, 2009

[8] M. Riera-Guasp, J. A. Antonino-Daviu, M. Pineda-Sanchez, R. Puche-Panadero, J. Perez-Cruz, "A General Approach for the Transient Detection of Slip-Dependent Fault Components Based on the Discrete Wavelet Transform," *IEEE Transactions on Industrial Electronics*, vol.55, no.12, pp.4167-4180, 2008

[9] B. Ayhan, M.-Y. Chow, M.-H. Song, "Multiple Discriminant Analysis and Neural-Network-Based Monolith and Partition Fault-Detection Schemes for Broken Rotor Bar in Induction Motors," *IEEE Transactions on Industrial Electronics*, vol.53, no.4, pp.1298-1308, 2006

[10] F. Filippetti, G. Franceschini, C. Tassoni, "Neural networks aided on-line diagnostics of induction motor rotor faults," *IEEE Transactions on Industry Applications*, vol.31, no.4, pp.892-899, 1995

[11] H. Razik, M. B. de Rossiter Corrêa, E. R. C. da Silva, "A Novel Monitoring of Load Level and Broken Bar Fault Severity Applied to Squirrel-Cage Induction Motors Using a Genetic Algorithm," *IEEE Transactions on Industrial Electronics*, vol.56, no.11, pp.4615-4626, 2009

[12] M. Haji, H. A. Toliyat, "Pattern Recognition - a Technique for Induction Machines Rotor Fault Detection eccentricity and Broken Bar Fault," *Proceedings of Industry Applications Annual Conference IAS*, vol.3, pp.1572-1578, 2001

[13] S. M. A. Cruz, H. A. Toliyat, A. J. Marques Cardoso, "DSP implementation of the multiple reference frames theory for the diagnosis of stator faults in a DTC induction motor drive," *IEEE Transactions on Energy Conversion*, pp.329-335, 2005

[14] S. M. A. Cruz, A. J. Marques Cardoso, "Rotor Cage Fault Diagnosis in Three-Phase Induction Motors, by Extended Park's Vector Approach," *Proceedings of International Conference on Electrical Machines*, pp.1844-1848, 1998

[15] M. Blödt, D. Bonacci, J. Regnier, M. Chabert, J. Faucher, "On-Line Monitoring of Mechanical Faults in Variable-Speed Induction Motor Drives Using the Wigner Distribution," *IEEE Transactions on Industrial Electronics*, pp.522-531, 2008

[16] E. Serna, J Pacas, 'Detection of Rotor Faults in Field Oriented Controlled Induction Machines', *Proceedings of IEEE Industry Applications Society Conference*, IAS vol.5, pp.2326-2332, 2006

[17] C. Kral, F. Pirker, G. Pascoli, H. Kapeller, "Robust Rotor Fault Detection by Means of the Vienna Monitoring Method and a Parameter Tracking Technique," *IEEE Transactions on Industrial Electronics*, vol.55, no.12, pp. 4229-4237, 2008

[18] S. M. Cruz, A. Stefani, F. Filippetti A. J. Marques Cardoso, "A New Model-Based Technique for the Diagnosis of Rotor Faults in RFOC Induction Motor Drives," *IEEE Transactions on Industrial Electronics*, vol.55, no.12, pp.4218-4228, 2008

[19] T. Wolbank, J. Machl, R. Schneiderbauer, "Detecting Rotor Faults in Inverter-Fed Induction Machines at Zero Load," *Proceedings of International Power Electronics and Motion Control Conference*, EPE-PEMC, Riga, Latvia, pp.1-6, 2004

[20] B. Kim, K. Lee, J. Yang, S. B. Lee, E. Wiedenbrug, M. Shah, "Automated detection of rotor faults for inverter-fed induction machines under standstill conditions," *IEEE Energy Conversion Congress and Exposition*, pp.2277-2284, 2009

[21] S. B. Lee, J. Yang, J. Hong, B. Kim, J. Yoo, K. Lee, J. Yun, M. Kim, K. Lee, E. J. Wiedenbrug, S. Nandi, "A New Strategy for Condition Monitoring of Adjustable Speed Induction Machine Drive Systems," *IEEE International Symposium on Diagnostics for Electric Machines, Power Electronics and Drives*, SDEMPED, pp.1-9, 2009

[22] C. Concari, G. Franceschini, C. Tassoni, "Self-commissioning procedures to detect parameters in healthy and faulty induction drives," *IEEE International Symposium on Diagnostics for Electric Machines, Power Electronics and Drives, SDEMPED*, pp.1-6, 2009

[23] T. Wolbank, P. Nussbaumer, H. Chen, P. Macheiner, 'Non-invasive detection of rotor cage faults in inverter fed induction machines at no load and low speed', *IEEE International Symposium on Diagnostics for Electric Machines, Power Electronics and Drives, SDEMPED*, pp.1-7, 2009